SCIENTIFIC REPORTS

OPEN

SUBJECT AREAS:
TWO-DIMENSIONAL MATERIALS
GRAPHENE
ELECTRONIC MATERIALS
NANOPARTICLES

Received
31 January 2013

Accepted
8 April 2013

Published
23 April 2013

Correspondence and requests for materials should be addressed to R.C.H. (haddon@ucr.edu)

Anisotropic Thermal and Electrical Properties of Thin Thermal Interface Layers of Graphite Nanoplatelet-Based Composites

Xiaojuan Tian[1,3], Mikhail E. Itkis[1,2], Elena B. Bekyarova[1,2] & Robert C. Haddon[1,2,3]

[1]Center for Nanoscale Science and Engineering, University of California - Riverside, Riverside, California 92521, USA, [2]Department of Chemistry, University of California - Riverside, Riverside, California 92521, USA, [3]Department of Chemical and Environmental Engineering, University of California - Riverside, Riverside, California 92521, USA.

Thermal interface materials (TIMs) are crucial components of high density electronics and the high thermal conductivity of graphite makes this material an attractive candidate for such applications. We report an investigation of the in-plane and through-plane electrical and thermal conductivities of thin thermal interface layers of graphite nanoplatelet (GNP) based composites. The in-plane electrical conductivity exceeds its through-plane counterpart by three orders of magnitude, whereas the ratio of the thermal conductivities is about 5. Scanning electron microscopy reveals that the anisotropy in the transport properties is due to the in-plane alignment of the GNPs which occurs during the formation of the thermal interface layer. Because the alignment in the thermal interface layer suppresses the through-plane component of the thermal conductivity, the anisotropy strongly degrades the performance of GNP-based composites in the geometry required for typical thermal management applications and must be taken into account in the development of GNP-based TIMs.

Thermal interface materials (TIMs) are crucial components of advanced high density electronic packaging and are necessary for the heat dissipation which is required to prevent the failure of electronic components due to overheating[1,2]. Conventional TIMs are manufactured by introducing highly thermally conductive fillers, like metal or metal oxide microparticles, into the polymer matrix[3–5]. With the rise of graphene[6], a product of graphite exfoliation[7,8], graphite nanoplatelets (GNPs), have been receiving significant attention as a new form of thermally conducting filler[9–24]. The GNPs are 2D high aspect ratio nanoparticles containing a few to hundreds of stacked graphene layers and because they possess the high in–plane thermal conductivity of graphite (~2,000 W/m*K), are expected to form a very efficient heat conduction pathway in polymer matrices. Indeed a tenfold enhancement of the thermal conductivity was achieved by adding only 5 to10 wt% of GNPs to the polymer matrix which allowed the preparation of composites with thermal conductivities up to 2 W/m*K[10–13,15,19,20,22,25], while conventional low aspect ratio fillers require a loading in the range of 60–90% to achieve a similar increase in the thermal conductivity[5]. With further increase of the GNP filler loading, composites with very high thermal conductivities (5–10 W/m*K) have been reported[10,11,14,24].

Most previous studies of GNP-based TIM composites have focused on the bulk thermal properties of macroscopic solid state specimens with a typical thickness of 2–10 mm, while practical thermal management applications require thin TIM layers with a bondline thickness of 10–100 μm, in a spreadable and conformable state which can completely fill the gap between the contacting surfaces while penetrating the crevices associated with the microscale surface roughness[2]. The TIM layer is expected to provide efficient heat flow from the die to the heat sink in the direction normal to the thermal interface as shown in Fig. 1a. Thus in such applications the ideal orientation of the GNPs is normal to the thermal interface plane which would take full advantage of the high in-plane thermal conductivity of graphite (Fig. 1b), whereas the isotropic, random (Fig. 1c) and parallel orientations (Fig. 1d) are expected to be much less favorable. In practice, the thin TIM layer is formed by spreading the material between the contacting surfaces under pressure or by underfilling the gap between parts by capillary flow[2,26,27]. During the spreading process the high aspect ratio of the GNPs could lead to their preferential orientation within the thermal interface layer (Fig. 1d), thus diminishing the contribution of the in-plane thermal conductivity of the

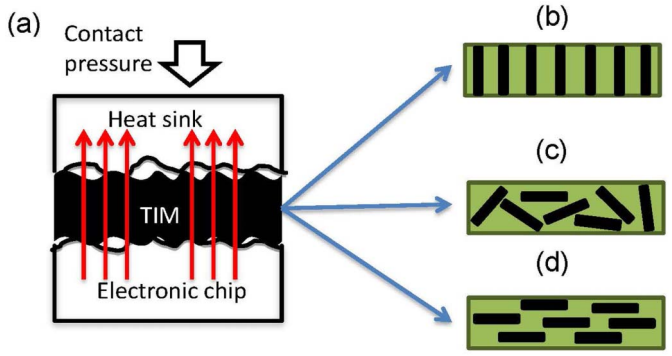

Figure 1 | Orientations of high aspect ratio GNP fillers in thin thermal interface layer in electronic packaging applications. (a) Schematic showing the utilization of thermal interface material layer for heat removal in electronic packaging. Possible orientations of GNPs in thin TIM layer: (b) preferentially through-plane, (c) isotropic, and (d) preferentially in-plane.

graphitic layers[16]. An extreme example of such in-plane orientation of GNPs was recently demonstrated by the preparation of a GNP paper which showed a highly anisotropic thermal conductivity, with an in-plane thermal conductivity of ~100 W/m*K, whereas the through-plane thermal conductivity was less than 1 W/m*K[17,28]. Similarly anisotropic heat conductance was recently demonstrated in boron nitride platelet thin films[29]. For practical application, GNP composite loadings in the range of 2–20 wt% are required but the orientational preferences of the GNPs in such composites has not been studied systematically and the thermal properties have often been assumed to be isotropic[30]. Here we report measurements which show a significant difference between the in-plane and through-plane electrical and thermal conductivities of thin layers of GNP-based thermal greases. We show that the anisotropic transport properties in the thin thermal interface layers originate from the preferential in-plane orientation of the GNPs and it is clear that the anisotropy of these composite matrices must be taken into account in the development of GNP based TIMs.

Results

In this study the GNPs were prepared by acid intercalation and thermal shock exfoliation according to previously published procedure[11,15,19,20]. Three commonly used matrices of differing viscosities and chemical nature, Epoxy 862 (Hexion, viscosity ν = 3050 cP), PMM 1025 silicon oil (Gelest, ν = 380 cP), and Hatcol 2372 (Hatco, ν = 234 cP), were used to produce GNP-based thermal greases with GNP loadings of 10–14 wt.%, denoted as GNP-Epoxy862, GNP-Silicon oil and GNP-Hatcol 2372, respectively (see Methods).

In-plane electrical conductivity measurements of thin (75 μm) layers of the thermal greases were conducted using the 4-probe technique (Fig. 2a, inset). The 4-probe technique is not viable for through-plane electrical conductivity measurements of thin grease layers, so we measured 2-probe electrical resistances of grease layers of three different thicknesses by sandwiching the grease between two gold coated glass slides (Fig. 2b, inset); this allows the calculation of the bulk through-plane electrical conductivity from the slope of the resistance as a function of thickness, which is linear in the thickness range 400–80 μm. The in-plane and through-plane electrical conductivity data for the three GNP-based greases are presented in Fig. 2(a, b). The results show that the in-plane and through-plane electrical conductivities of the GNP composites differ by several orders of magnitude. The in-plane electrical conductivity increases from $\sigma_{\|}$ = 2.4 to 4 S/cm with decreasing viscosity of the polymer matrix (Fig. 2a), whereas the through-plane conductivity ($\sigma_{\perp}$) shows the opposite behavior (Fig. 2b), and never exceeds 0.01 S/cm. Thus the electrical anisotropy increases with decreasing viscosity of the polymer and exceeds 1000 in the case of the low viscosity Hatco 2372 matrix (Fig. 2c); these values are much higher than the anisotropies (~10) reported for bulk GNP-based composites[23,31].

The experimental setups for the through-plane and in-plane thermal conductivity measurements are presented in Fig. 3a and Fig. 3b, respectively. The through-plane thermal conductivity of the GNP based grease layers of thicknesses 100 to 300 μm was measured with a LW-9389 TIM Tester (Longwin, Taiwan) which operates on the basis of the steady-state heat flow technique according to ASTM D5470-06. In this technique, the bulk through-plane thermal conductivity is calculated from the slope of the thermal resistance versus thickness, which was observed to be linear in the thickness range 300–100 μm. The through-plane thermal conductivities $\kappa_{\perp}$ of GNP-Silicon oil, GNP-Hatcol 2372 and GNP-Epoxy862 composites at the same filler loading (14 wt.%) are presented in Fig. 3e and show a decrease of $\kappa_{\perp}$ with decreasing viscosity similar to the case of the through-plane electrical conductivity (Fig. 2b). Typical values of the through-plane thermal conductivity were $\kappa_{\perp}$ = 0.5–0.9 W/m*K for GNP loading between 11 and 14 wt.%. (Fig. 3e,f). The in-plane thermal conductivity ($\kappa_{\|}$) of the GNP composite was measured by utilizing a comparative technique which was previously applied to the measurement of the thermal conductivities of carbon nanotube (CNT) bundles and CNT-epoxy composites[32-34]. This technique is not fully transferable to the grease samples and we found it necessary to cure the greases under pressure at elevated temperature, which resulted in thin film samples of thickness 100 to 300 μm. In order to preserve the GNP orientation throughout the curing, the processing conditions of the thin film were designed to mimic the parameters adopted in the TIM tester. As an internal check, Fig. 3f includes data for both the in-plane ($\kappa_{\|}$) and through-plane ($\kappa_{\perp}$) thermal conductivities of the cured (solid film) specimens, together with results obtained on the grease samples.

Fig. 3b shows the schematics and an image of the experimental implementation of the comparative technique. The in-plane oriented sample with lateral dimensions of 6 × 2 mm^2 and thickness ~200 μm was cut from the cured GNP film. A thermal gradient was imposed by a miniature thermoelectric stage so as to direct the heat flow through the GNP sample and the 0.5 mm diameter constantan wire of known thermal conductivity (19.5 W/m*K), which were mounted in series. The sign of the temperature gradient was alternated by reversing the voltage at the thermoelectric stage and the results of the oppositely polarized measurements were averaged to exclude any contribution from black body radiation. Representative results from the experiments are included in Fig. 3d in the form of the temperature gradients as a function of polarity. Measurements of several thin film samples gave value for the in-plane thermal conductivity of the GNP-based TIM layer of $\kappa_{\|}$ = 4.5 ± 0.5 W/m*K (Fig. 3f) corresponding to an anisotropy in the thermal conductivity of ~5, which is very significant for TIM applications.

The electrical and thermal measurements show anisotropic electron and phonon transport in thin TIM layers which may originate from the preferential in-plane orientation of the GNPs; in order to directly address this question, we conducted SEM studies of the cross-sections of the GNP films. The clean GNP film cross-sections were prepared by immersing the film in liquid nitrogen and breaking it in a frozen state by applying a shear force[31]; the resulting images are presented in Fig. 4 and clearly indicate preferential in-plane orientation of the GNPs, thereby providing an obvious rationale for the observed anisotropy of the electrical and thermal conductivities.

Discussion

The present measurements show strongly anisotropic electron and phonon transport in GNP-based thin TIM layers and the SEM study directly associates the observed anisotropy with the preferential in-plane alignment of the GNPs established during lateral flow of the

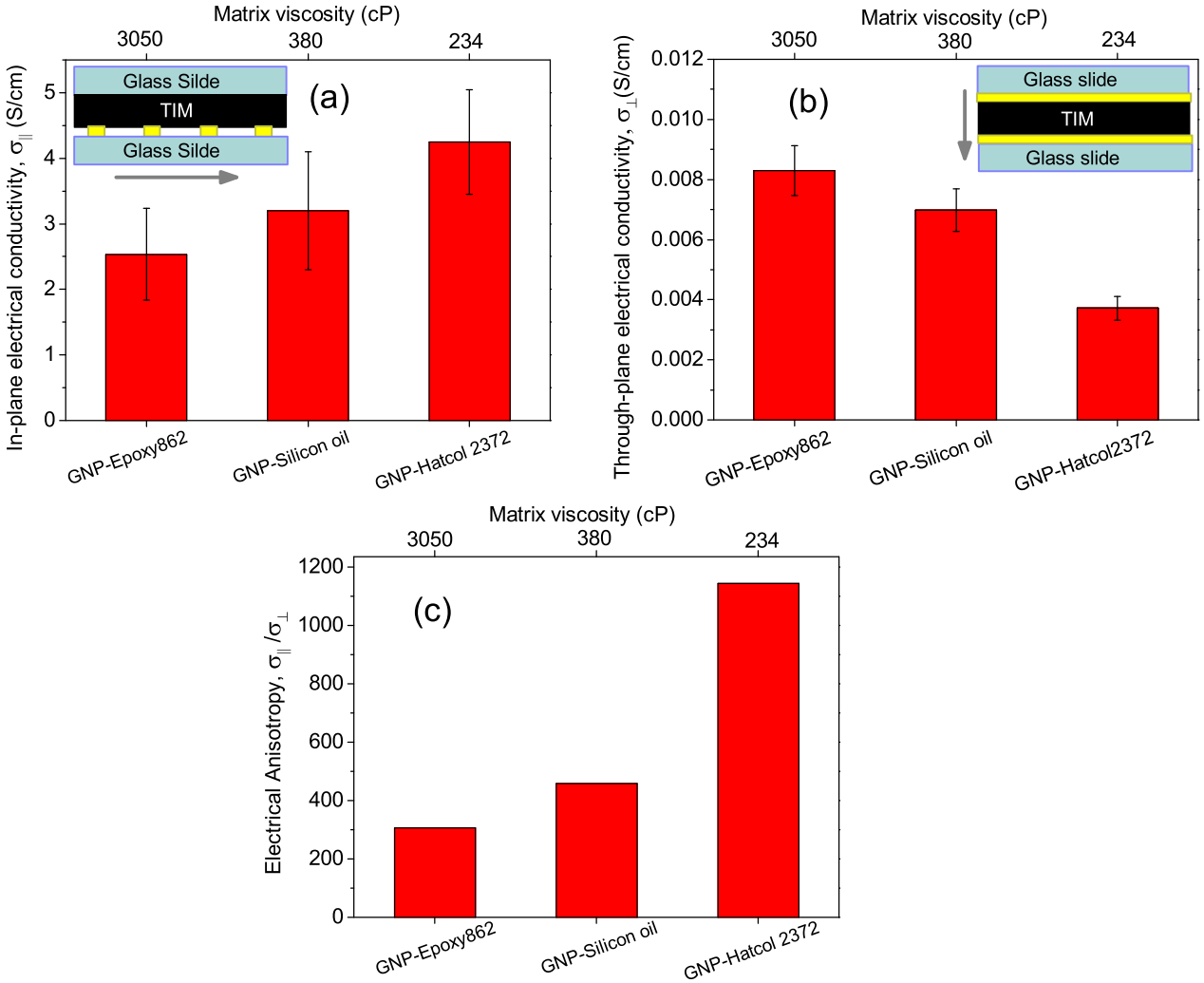

Figure 2 | Measurements of anisotropic electrical conductivity in GNP-based thin thermal interface layers. (a) In-plane $\sigma_{\parallel}$ and (b), through-plane $\sigma_{\perp}$ electrical conductivities of GNP-based greases for matrices of different viscosities at GNP loading 14 Weight%, and (c) anisotropy values $\sigma_{\parallel}/\sigma_{\perp}$.for these greases. Insets in Fig. 2a and Fig. 2b show electrode configuration utilized for the in-plane and through-plane electrical measurements, respectively.

GNP-based grease under applied pressure. The increase in the anisotropy of the electrical conductivity with decreasing viscosity of the polymer matrix (Fig. 2) suggests that at low viscosities the polymer matrix is unable to resist the natural alignment of the GNPs. The decrease of the through-plane thermal conductivity with decreasing viscosity of the polymer matrix (Fig. 3e) provides additional support for this interpretation. The thermal anisotropy is about two orders of magnitude smaller than the electrical anisotropy; this difference is not surprising taking into account the fact that the electrical conductivities span a range of more than 30 orders of magnitude between the best electrical conductors such as copper ($\sigma \approx 6 \times 10^5$ S/cm) and electrical insulators such as Teflon ($\sigma \approx 10^{-26}$ S/cm), while the difference between the best thermal conductors such as graphite (~2000 W/m*K) and copper (~400 W/m*K), and thermal insulators such as Teflon (~0.25 W/m*K) is only 5 orders of magnitude[35,36]. This can be explained by the fact that electronic component contributes to both electrical and thermal transport with approximately the same span of the ranges while the phonon component contributes only to thermal transport thus increasing the thermal conductivity and reducing the contrast between thermally conductive and thermally insulating materials[34,35].

The quality of TIMs is typically evaluated by measurement of the thermal interface resistance R_{TIM}, which depends on the bulk thermal conductivity of TIM, the bond line thickness (BLT) of the TIM layer and the contact resistance R_C between the TIM and the contacting surfaces[37]. The thermal interface resistance can be decreased by increasing the bulk thermal conductivity of the TIM, reducing the BLT or reducing the contact resistance between the chip and heat sink[27]. Current commercially available thermal interface materials provide R_{TIM} in the range 0.1–0.4°C*cm²/W[37–39], whereas it is anticipated that in the future, electronic packaging will require R_{TIM} in the range 0.05–0.01°C*cm²/W and a BLT in the range 10–50 μm. Based on a BLT = 20 μm, the required bulk thermal conductivity should be > 4 W/m*K which is in the range of the measured in-plane thermal conductivity of GNP based TIMs, but much higher than the current through-plane values.

As we discussed above, the TIM layer is expected to provide efficient heat flow from the die to the heat sink in the direction normal to the thermal interface (Fig. 1a), but we found that orientation of the GNPs follows the in-plane alignment pattern illustrated in Fig. 1d, in contrast to ideal orientation of the GNPs normal to the thermal interface plane (Fig. 1b); the latter orientation would take full advantage of the high in-plane thermal conductivity of graphite although the isotropic, random orientation of GNPs (Fig. 1c) would be also acceptable. We suggest that the observed thermal anisotropy imposes a significant limitation on the performance of GNP fillers as the

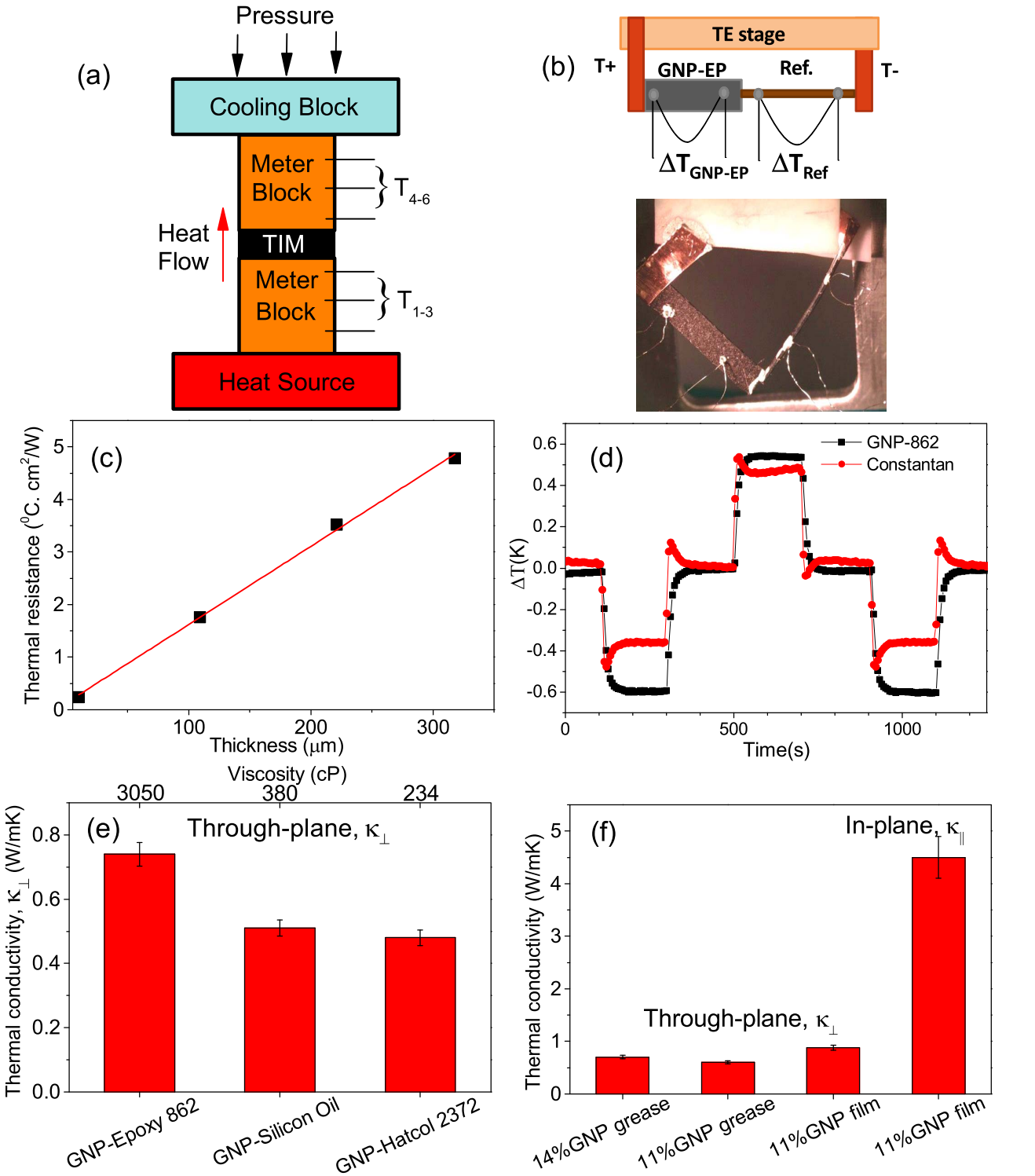

Figure 3 | Measurements of anisotropic thermal conductivity in GNP-based thin thermal interface layers. (a) Schematic of TIM Tester for through-plane thermal conductivity measurements; (b) Schematic of the setup for in-plane thermal conductivity measurements of GNP-epoxy thin films by use of the comparison technique, and its experimental realization; (c) Thermal resistance as a function of thickness for the determination of through-plane thermal conductivity of thin TIM layers; (d) Thermal pulses along the GNP-epoxy thin film (red circles) and reference constantan wire (black squares) recorded during comparative technique data acquisition; (e) Through-plane ($\kappa_{\perp}$) thermal conductivities of GNP based greases for polymer matrices of different viscosities; (f) Through-plane ($\kappa_{\perp}$) and in-plane ($\kappa_{\parallel}$) thermal conductivities of thin GNP-epoxy layers.

through-plane heat dissipation is crucial in thermal management applications; thus further practical advancements in this field will probably require the disruption of the in-plane orientation of the two-dimensional GNPs. Because the alignment in the thermal interface layer suppresses the through-plane component of the thermal conductivity, the anisotropy acts to strongly degrade the performance of the GNP-based composites in the geometry required for typical thermal management applications and must be taken into account in the future development of GNP-based thermal interface materials.

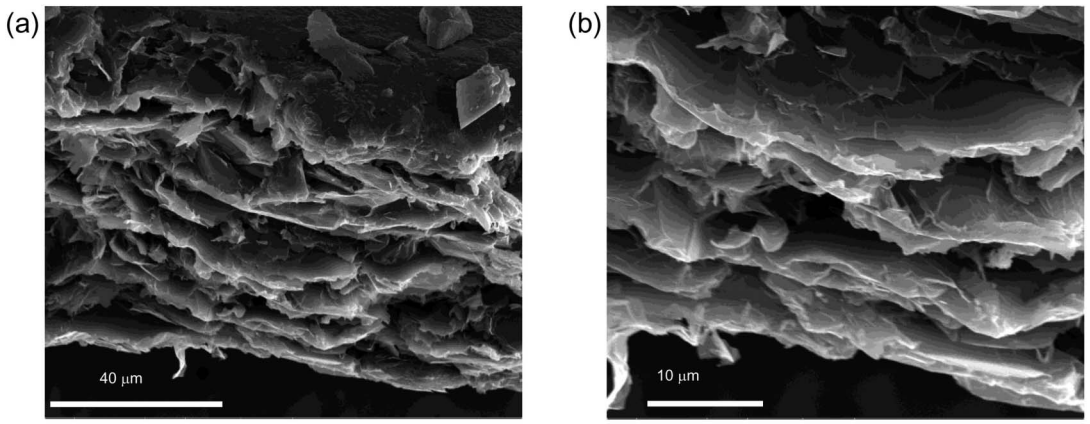

Figure 4 | SEM study of GNP filler orientation in thin thermal interface layers. SEM images of the cross-section of a thin layer of the GNP-epoxy composite thin film at different magnifications with scale bars: (a) 40 μm and (b) 10 μm.

Methods

Preparation of GNPs based thermal grease. In a typical experiment, 10 g of natural graphite (TIMCAL Graphite and Carbon, Inc.) were treated for 12 hours at room temperature with a 120 mL mixture of concentrated sulfuric and nitric acids (3 : 1). The intercalated graphite was filtered, washed with distilled water, air dried, and exfoliated in an oven at 800°C for 3 min under flow of argon. The exfoliated graphite was dispersed in acetone by high shear mixing for 30 min followed by bath sonication for 24 h to produce a GNP dispersion. The polymers were added to the GNPs dispersions, high shear mixed for 30 minutes followed by removal of the solvent. The resulting mixtures were processed utilizing a dual asymmetric centrifuge Speed Mixer (DAC 150.1 FVZ, Flack Tek, Inc.) to produce homogeneous and spreadable thermal greases of a consistency which is typical of TIMs that are suitable for application. To prepare cured samples the curing agent (EPI-CURE W, Hexion) was added to the GNP-Epoxy 862 grease (1 : 4 ratio), the mixture was heated under a pressure of 40 psi at 80°C for 2 h, 100°C for 2 h and 150°C for 2.5 h to obtain thin films of thickness 100 to 300 μm.

Electrical conductivity measurement. For the in-plane electrical conductivity measurements the thermal greases were spread into a thin (75 μm) layer between two glass slides under a pressure of 40 psi at a temperature of 60°C, which is typical for TIM applications. The bottom slide was patterned with 4 in-line gold electrodes positioned 5 mm apart for 4-point electrical measurements (Fig. 2a, inset). For through-plane electrical conductivity measurements 2-probe technique was applied; we measured the electrical resistances of three grease layers with thicknesses between 50 and 400 μm by sandwiching the grease layer between two gold coated glass slides (Fig. 2b, inset) at the same pressure (40 psi) and temperature (60°C), which allows the calculation of the bulk through-plane electrical conductivity from the slope of the resistance as a function of thickness, thereby excluding the contact resistance.

Thermal conductivity measurement. The through-plane thermal conductivity of the GNP based greases was measured in the temperature range 30–60°C with a LW-9389 TIM Tester (Longwin, Taiwan) utilizing the steady-state heat flow technique according to ASTM D5470-06. The heat flow and the temperature across the TIM layer was measured utilizing a set of precision thermometers positioned in the Copper metal blocks along the direction of the thermal gradient (Fig. 3a). The thermal resistances were measured for 3-4 thicknesses of the thermal grease layer (10 to 300 μm), and the bulk thermal conductivity of the grease was extracted from a plot of the resistance against thickness, thereby excluding the contact resistance (Fig. 3c). The thermal conductivities of the polymer matrices Epoxy 862, PMM 1025 silicon oil and Hatcol 2372 measured by this technique were 0.15, 0.15 and 0.13 W/m*K, respectively. The in-plane thermal conductivity ($\kappa_{||}$) of the GNP composite was measured in the temperature range 30–40°C by utilizing a comparative technique[32–34]. A thermal gradient was imposed by a miniature thermoelectric stage so as to direct the heat flow through the GNP sample and the 0.5 mm diameter constantan wire of known thermal conductivity (19.5 W/m*K, reference sample), which were mounted in series. Miniature differential thermocouples were utilized to measure the temperature gradients across the GNP and the reference sample. The sign of the temperature gradient was alternated by reversing the voltage at the thermoelectric stage and the results of the two polarity measurements were averaged in order to exclude any contribution to the heat loss originating from the black body radiation emanating from the sample. This freedom to invert the sign of the temperature gradient allowed us to position the same reference either before or after the sample with respect to the direction of heat flow, thereby measuring the heat flow entering or exiting the sample before or after the occurrence of radiative heat loss which is equivalent to using two references – a common practice in the comparative technique[32–34]. The experiment was enclosed in a vacuum chamber operating at a pressure of 10^{-6} Torr, and was tested on samples of known thermal conductivity.

Viscosity measurements. The viscosity of the polymer matrices were measured using a Brookfield DV-II+Pro viscometer.

SEM study. SEM study was conducted utilizing Nova NanoSEM 450 instrument (FEI Company). The clean GNP film cross-sections were prepared by immersing the film in liquid nitrogen and breaking it in a frozen state by applying a shear force[31].

1. Schelling, P. K., Shi, L. & Goodson, K. E. Managing heat for electronics. *Mater. Today* **8**, 30–35 (2005).
2. Prasher, R. Thermal interface materials: historical perspective, status, and future directions. *Proc. IEEE* **94**, 1571–1586 (2006).
3. Xu, Y. S. & Chung, D. D. L. Increasing the thermal conductivity of boron nitride and aluminum nitride particle epoxy-matrix composites by particle surface treatments. *Compos. Interfaces* **7**, 243–256 (2000).
4. Prasher, R. S., Shipley, J., Prstic, S., Koning, P. & Wang, J. L. Thermal resistance of particle laden polymeric thermal interface materials. *ASME J. Heat Transfer* **125**, 1170–1177 (2003).
5. Lu, D., Wong, C. P., Prasher, R. & Chiu, C. P. *Materials for Advanced Packaging* 437–458 (Springer US, 2009).
6. Geim, A. K. & Novoselov, K. S. The rise of graphene. *Nature Mater.* **6**, 183–191 (2007).
7. Dresselhaus, M. S., Dresselhaus, G., Eklund, P. C. & Chung, D. D. L. Lattice-vibrations in graphite and intercalation compounds of graphite. *Mater. Sci. Eng.* **31**, 141–152 (1977).
8. Chung, D. D. L. Exfoliation of graphite. *J. Mater. Sci.* **22**, 4190–4198 (1987).
9. Yasmin, A. & Daniel, I. M. Mechanical and thermal properties of graphite platelet/epoxy composites. *Polymer* **45**, 8211–8219 (2004).
10. Fukushima, H., Drzal, L. T., Rook, B. P. & Rich, M. J. Thermal conductivity of exfoliated graphite nanocomposites. *J. Therm. Anal. Calorim.* **85**, 235–238 (2006).
11. Yu, A., Ramesh, P., Itkis, M. E., Bekyarova, E. & Haddon, R. C. Graphite nanoplatelet-epoxy composite thermal interface materials. *J. Phys. Chem. C* **111**, 7565–7569 (2007).
12. Kalaitzidou, K., Fukushima, H. & Drzal, L. T. Multifunctional polypropylene composites produced by incorporation of exfoliated graphite nanoplatelets. *Carbon* **45**, 1446–1452 (2007).
13. Debelak, B. & Lafdi, K. Use of exfoliated graphite filler to enhance polymer physical properties. *Carbon* **45**, 1727–1734 (2007).
14. Ganguli, S., Roy, A. K. & Anderson, D. P. Improved thermal conductivity for chemically functionalized exfoliated graphite/epoxy composites. *Carbon* **46**, 806–817 (2008).
15. Yu, A. *et al.* Enhanced thermal conductivity in a hybrid graphite nanoplatelet - carbon nanotube filler for epoxy composites. *Adv. Mater.* **20**, 4740–4744 (2008).
16. Lin, C. & Chung, D. D. L. Graphite nanoplatelet pastes vs. carbon black pastes as thermal interface materials. *Carbon* **47**, 295–305 (2009).
17. Veca, L. M. *et al.* Carbon nanosheets for polymeric nanocomposites with high thermal conductivity. *Adv. Mater.* **21**, 2088–2092 (2009).
18. Kim, S. & Drzal, L. T. High latent heat storage and high thermal conductive phase change materials using exfoliated graphite nanoplatelets. *Sol. Energy Mater. Sol. Cells* **93**, 136–142 (2009).
19. Sun, X., Ramesh, P., Itkis, M. E., Bekyarova, E. & Haddon, R. C. Dependence of the thermal conductivity of two-dimensional graphite nanoplatelet-based composites on the nanoparticle size distribution. *J. Phys.: Condens. Matter* **22**, 334216–334219 (2010).
20. Sun, X. *et al.* Oxidized graphite nanoplatelets as an improved filler for thermally conducting epoxy-matrix composites. *J. Electron. Packaging* **133**, 020905 (2011).

21. Yavari, F. *et al.* Enhanced thermal conductivity in a nanostructured phase change composite due to low concentration graphene additives. *J. Phys. Chem. C* **115**, 8753–8758 (2011).
22. Raza, M. A., Westwood, A., Brown, A., Hondow, N. & Stirling, C. Characterisation of graphite nanoplatelets and the physical properties of graphite nanoplatelet/silicone composites for thermal interface applications. *Carbon* **49**, 4269–4279 (2011).
23. Raza, M. A., Westwood, A. & Stirling, C. Carbon black/graphite nanoplatelet/rubbery epoxy hybrid composites for thermal interface applications. *J. Mater. Sci.* **47**, 1059–1070 (2012).
24. Shahil, K. M. F. & Balandin, A. A. Graphene-multilayer graphene nanocomposites as highly efficient thermal interface materials. *Nano Lett.* **12**, 861–867 (2012).
25. Xiang, J. & Drzal, L. T. Investigation of exfoliated graphite nanoplatelets (xgnp) in improving thermal conductivity of paraffin wax-based phase change material. *Sol. Energy Mater. Sol. Cells* **95**, 1811–1818 (2011).
26. Kooi, C. C. *et al.* Capillary underfill and mold encapsulation materials for exposed die flip chip molded matrix array package with thin substrate, *EPTC*, 324–330 (2003).
27. Samson, E. C. *et al.* Interface material selection and a thermal management technique in second-generation platforms built on Intel® Centrino™ mobile technology. *Intel Tech. J.* **09**, 75–86 (2005).
28. Xiang, J. L. & Drzal, L. T. Thermal conductivity of exfoliated graphite nanoplatelet paper. *Carbon* **49**, 773–778 (2011).
29. Song, W. L. *et al.* Polymer/boron nitride nanocomposite materials for superior thermal transport performance. *Angew. Chem. Int. Ed.* **51**, 6498–6501 (2012).
30. Li, J. & Kim, J. K. Percolation threshold of conducting polymer composites containing 3d randomly distributed graphite nanoplatelets. *Compos. Sci. Technol.* **67**, 2114–2120 (2007).
31. Raza, M. A., Westwood, A. V. K., Brown, A. P. & Stirling, C. Texture, transport and mechanical properties of graphite nanoplatelet/silicone composites produced by three roll mill. *Compos. Sci. Technol.* **72**, 467–475 (2012).
32. Hone, J. *et al.* Electrical and thermal transport properties of magnetically aligned single wall carbon nanotube films. *Appl. Phys. Lett.* **77**, 666–668 (2000).
33. Biercuk, M. J. *et al.* Carbon nanotube composites for thermal management. *Appl. Phys. Lett.* **80**, 2767–2769 (2002).
34. Tritt, T. M. (ed.) *Thermal Conductivity: Theory, Properties and Applications.* (Kluwer Academic/Plenum Publishers, New York, New York; 2004).
35. Shenogina, N., Shenogin, S., Xue, L. & Keblinski, P. On the lack of thermal percolation in carbon nanotube composites. *Appl. Phys. Lett.* **87**, 133106 (2005).
36. Itkis, M. E., Borondics, F., Yu, A. & Haddon, R. C. Thermal conductivity measurement of semitransparent single-walled carbon nanotube films by a bolometric technique. *Nano Lett.* **7**, 900–904 (2007).
37. Gwinn, J. P. & Webb, R. L. Performance and testing of thermal interface materials. *Microelectron. J.* **34**, 215–222 (2003).
38. Narumanchi, S., Mihalic, M., Kelly, K. & Eesley, G. Thermal interface materials for power electronics applications. *ITHERM* **11**, 395–404 (2008).
39. Liu, J. *et al.* Recent progress of thermal interface material research - an overview. *THERMINIC* **14**, 156–162 (2008).

Acknowledgements

This material is based on research sponsored by DARPA/Defense Microelectronics Activity (DMEA) under agreement number H94003-10-2-1004. The United States Government is authorized to reproduce and distribute reprints for Government purposes, notwithstanding any copyright notation thereon. The SEM imaging was performed at CFAMM – University of California-Riverside.

Author contributions

X.T., M.I. and R.C.H. contributed to the original idea. M.I. and R.C.H. supervised the project. X.T. and M.I. designed and set up the experiment. X.T. performed the experiment. X.T., M.I., E.B. and R.C.H. contributed to the data analysis, interpretation of the results and preparation of the manuscript. M.I. and R.C.H. wrote the manuscript.

Additional information

Competing financial interests: The authors declare no competing financial interests.

How to cite this article: Tian, X., Itkis, M.E., Bekyarova, E.B. & Haddon, R.C. Anisotropic Thermal and Electrical Properties of Thin Thermal Interface Layers of Graphite Nanoplatelet-Based Composites. *Sci. Rep.* **3**, 1710; DOI:10.1038/srep01710 (2013).